Molecular Motion of Poly(methyl methacrylate) Chains Tethered on a Poly(tetrafluoroethylene) Surface

Katsuhiro Yamamoto,* Shigetaka Shimada, and Yoshiharu Tsujita

Nagoya Institute of Technology, Gokiso-cho, Showa-ku, Nagoya 466, Japan

Masato Sakaguchi

Ichimura Gakuen College, 61, Uchikubo, Inuyama 484, Japan

Received May 16, 1996; Revised Manuscript Received November 19, 1996[⊗]

ABSTRACT: Poly(methyl methacrylate) (PMMA) chains were graft-copolymerized on a poly(tetrafluoroethylene) (PTFE) surface, and the tethered PMMA chains were spin-labeled to study the molecular motion of the PMMA chains by electron spin resonance (ESR). Two spectral components, a "fast" (isotropic) and a "slow" (anisotropic) component, with different rates of motion were observed in a certain temperature range. The isotropic and anisotropic components of the ESR spectra are identified with the fast and slow regions of polymer chain motion, respectively. Two transition temperatures, T_L and T_H, and the difference between T_L and T_H, ΔT, were estimated. The lower T_L is where the sharp ^{14}N isotropic triplet spectrum first appears as the sample is warmed, while the upper T_H is where the broad spectrum identified with the anisotropic pattern finally disappears. It was found that the transition temperatures and the ΔT of the tethered PMMA chains increased, had maximum values around ca. 3% grafting ratio, and decreased toward the transition temperatures and the ΔT of PMMA homopolymer chains with an increase in grafting ratio. The T_L for the sample with 1.2% grafting ratio is about 40 K lower than that for PMMA homopolymer, whereas the T_H for the grafting sample is 30 K higher than that for the homopolymer. These facts reflect a wide distribution of molecular structure of the tethered chains. The mobile chains protrude from the PTFE surface and have an extremely low segmental concentration of the PMMA molecules. On the other hand, the rigid chains take an entangled structure and are adsorbed on the PTFE surface.

Introduction

Many investigations on the molecular motion of polymer chains in the solid state have been reported by ESR.[1−5] The intermolecular (intersegment) interaction is an important factor for the molecular motion. Each of the polymer chains in the bulk is surrounded by the other chains and then has a limited space that reflects its molecular mobility.

In order to clarify the intermolecular interaction related to the molecular motion, we study the molecular mobility of the polymer chains tethered on the other solid polymer surface as a function of grafting ratio. The grafting ratio should be related to the segmental concentration and intermolecular interaction of the tethered polymer chains, assuming that the tethered chains are immiscible with the surface polymer chains.

We investigated the molecular motion of the chain end radical of polyethylene (PE) tethered on the PTFE surface by ESR and reported that the chain end radical has a high mobility even at 77 K because of a weak interaction between PE and PTFE composing the surface and an extremely low segmental density of the PE chains.[6,7] Moreover, we clarified that the PE chain tethered on the PTFE surface has a high mobility by means of peroxy radical end-labeling.[8] We could not obtain a sample of PE graft copolymer chains on PTFE (PTFE-*g*-PE) with a high grafting ratio, and thus we could not qualitatively estimate the molecular mobility of the tethered polymer chains in a wide range of grafting ratio.

In this paper, however, we prepare samples of PMMA graft copolymer chains on PTFE (PTFE-*g*-PMMA) with a wide range of grafting ratio. We will report the molecular motion of the PMMA chains tethered on the PTFE surface as a function of grafting ratio related to segmental density and discuss a mechanism of the molecular motion of the PMMA chains.

Experimental Section

Materials. Poly(tetrafluoroethylene) powder (Fluon G163, Asahi Glass Co., Ltd.) was used without further purification. Atactic-PMMA ($M_w = 83\,000$ $M_w/M_n = 1.85$) (Aldrich Chemical Co., Inc.) was purified by dissolving in acetone, precipitating in excess methanol, and filtering. This procedure was repeated three times. The PMMA powder sample was then dried *in vacuo* at room temperature for 2 days. MMA monomer (Nacalai Tesque, Inc.) was purified as usual by a freeze−pump−thaw method.

Preparation of PMMA Chains Tethered on a PTFE Surface. (1) The mechanical fractures of PTFE powder (1.5 g) with MMA monomer (0.5 mL) were carried out by milling in a homemade vibration glass ball mill *in vacuo* at room temperature for 4, 8, and 24 h.[9] PMMA chains tethered on the PTFE surface were produced by block (graft) copolymerization of MMA monomer, which was initiated by the PTFE mechanoradicals trapped on the PTFE surface.[9,10] After milling, unreacted monomer and PMMA homopolymer were extracted with acetone using a Soxhlet apparatus. These samples are named PTFE/MMA(4h), PTFE/MMA(8h), and PTFE/MMA(24h) for 4, 8, and 24 h milling, respectively.

(2) PTFE powder irradiated with γ-rays (13 kGy) in air was placed in glass tubes and degassed. After the introduction of MMA monomer to these glass tubes, these were sealed and placed at 343 K for 2 and 6 h to produce PMMA chains tethered on the PTFE surface.[11] This graft copolymerization was initiated by radicals on the PTFE surface. After the copolymerization, unreacted monomer and PMMA homopolymer were removed. These samples are named γ-PTFE/MMA-(2h) and γ-PTFE/MMA(6h) for 2 and 6 h copolymerization, respectively.

Spin-Labeling. The tethered PMMA chains and the PMMA homopolymer were spin-labeled by amide−ester interchange reaction with 2,2,6,6-tetramethyl-4-aminopiperi-

[⊗] Abstract published in *Advance ACS Abstracts,* February 15, 1997.

S0024-9297(96)00718-8 CCC: $14.00

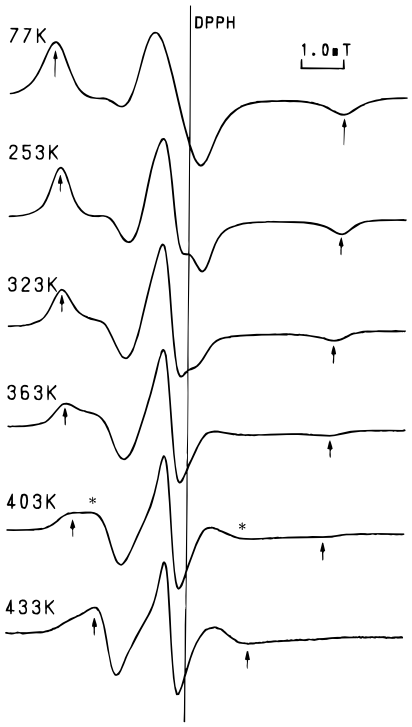

Figure 1. ESR spectra of S-PMMA observed at various temperatures. The separation between arrows shows the extreme separation width.

dine-1-oxyl (4-amino-TEMPO) (Aldrich) in methanol containing sodium methoxide.[12,13] The labeled samples were repeatedly dispersed in $CH_3OH \cdot H_2O$ and filtered to remove the large amount of unreacted spin-label reagents. This procedure was repated more than six times. As discussed in the following section, it can be considered that the PMMA chains on the surface of the bulk were selectively spin-labeled because the reaction was performed in a poor solvent for PMMA. This PMMA sample is named S-PMMA.

Determination of Grafting Ratio. The grafting ratio of each sample was determined by thermogravimetry (TG) using a TG8101D (Rigaku Denki) and taking advantage of the different range of degradation temperatures between PMMA (around 580−650 K) and PTFE (around 780−840 K). A heating rate of 5 K/min was used. The grafting ratio was calculated by the following equation:

$$\text{grafting ratio (\%)} = \frac{\text{PMMA fraction (g)}}{\text{PTFE fraction (g)}} \times 100$$

ESR Measurements. ESR spectra were observed *in vacuo* at a low microwave power level to avoid power saturation and with 100 kHz field modulation using JEOL JES-FE3XG at 77 K and JES-RE1XG spectrometers above 113 K (X-band) coupled to a microcomputer (NEC PC-9801). The signal of DPPH (1,1-diphenyl-2-picrylhydrazyl) was used as a *g*-value standard. The magnetic field was calibrated with the well-known splitting constants of Mn^{2+} in MgO.

Results and Discussion

Surface Molecular Mobility of PMMA Homopolymer. Figure 1 shows the ESR spectra of S-PMMA observed at various temperatures. In general, the outermost splitting width of the main triplet spectrum due to hyperfine coupling caused by the nitrogen nucleus narrows with an increase in mobility of the radicals becuase of motional averaging of the anisotropic interaction between electron and nucleus. The complete averaging gives rise to the isotropic narrowed spectrum. The extreme separation width between arrows indicated in Figure 1 gradually narrows with an increase in temperature. New humps indicated with the asterisks appear at 373 K and two spectral components, a "fast" and a "slow" component, are observed in a certain temperature range. The slow component with the large outermost splitting width and the fast component with the new humps can be attributed to radicals in the rigid and mobile region, respectively.

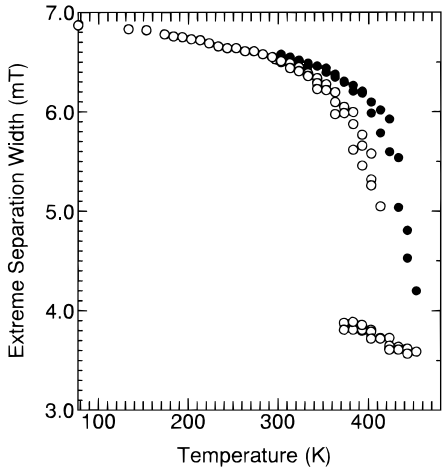

Figure 2. Temperature dependencies of the extreme separation width for S-PMMA (○) and B-PMMA (●).

The temperature dependence of the extreme separation width for the S-PMMA sample is shown in Figure 2 (open circles). The transition temperature at which an extreme separation width equal to 5.0 mT is defined as $T_{5.0mT}$. Tsay et al. reported the $T_{5.0mT}$ of atactic-PMMA homopolymer to be 450 K.[4] Sohma et al. also reported the $T_{5.0mT}$ of isotactic-PMMA homopolymer to be about 420 K.[1] In the case of S-PMMA, the $T_{5.0mT}$ is about 410 K. It is approximately 40 K lower than the $T_{5.0mT}$ obtained by Tsay et al. The low $T_{5.0mT}$ may be attributed to the spin-labeled PMMA chains located near the surface because the spin-label reaction was performed in a poor solvent for PMMA. In order to confirm the trapping region of the spin-labeled PMMA chains, an additional experiment was executed. The sample of S-PMMA was dissolved in benzene and precipitated in methanol. By this procedure, the spin-labeled PMMA chains located on the surface should diffuse into the interior region. This sample is named B-PMMA. The temperature dependence of the extreme separation width for this sample is shown in Figure 2 (solid circles) and the $T_{5.0mT}$ results in about 440 K, which nearly equals the $T_{5.0mT}$ reported by Tsay et al. Thus, the spin-labeled PMMA in the S-PMMA sample can be confirmed to be located near the surface. The $T_{5.0mT}$ of S-PMMA is 30 K lower than that of B-PMMA. This is evidence that the molecular mobility is higher on the surface than in the interior. These experimental facts suggest that segmental distributions near a surface for PMMA are different from the bulk profile;[14,15] i.e., the segmental density near the surface is lower than that in the interior. Two spectral components observed for S-PMMA can be interpreted in terms of a distribution of correlation times arising from a distribution of the segmental density near the surface.

Molecular Motion of PMMA Chains Tethered on the Surface of PTFE. (a) Characterization of Tethered PMMA Chains. The characteristics for PTFE-*g*-PMMA samples are summarized in Table 1.

The tethered point concentration was determined as follows: In the case of mechanically fractured samples, PTFE powder (1.5 g) was fractured with MMA monomer

Table 1. Characteristics of PTFE-*g*-PMMA Samples

sample name	grafting ratio (%)	tethered point concn (spin/g)	area per tethered point (Å^2/point) (A)	av deg of polymerization; DP	$2\langle S^2\rangle^{1/2}$	$2\langle S^2\rangle^{1/2}/A^{1/2}$
PTFE/MMA(4h)	0.1	2.9×10^{15}	7.2×10^4	2.1×10^3	81	0.3
PTFE/MMA(8h)	1.2	3.6×10^{15}	5.8×10^4	2.0×10^4	250	1.0
PTFE/MMA(24h)	2.7	5.8×10^{15}	3.6×10^4	2.8×10^4	300	1.6
γ-PTFE/MMA(2h)	10	2.7×10^{17}	7.8×10^2	2.2×10^3	83	3.4
γ-PTFE/MMA(6h)	30	2.7×10^{17}	7.8×10^2	6.5×10^3	140	5.0

(0.5 mL) and nitrosobenzene (0.02 g), and then the absolute concentration of the produced nitroxide radicals was estimated by ESR. The ratio of the amount of PTFE to that of MMA monomer is just same as that described in the Experimental Section. Assuming that nitrosobenzene can trap all of the mechanoradicals produced by the milling and/or the propagating radicals of PMMA, the tethered point concentration and the area per tethered point (denoted as A) should be calculated using the specific surface area, 2.1 m^2/g, of the PTFE powder.[7] In the case of the γ-ray-irradiated sample, a toluene solution containing DPPH (0.4 mg/L) was added to the irradiated PTFE, and the sample was incubated in a sealed tube at 343 K for 2 h. The determination of the amount of the DPPH radicals reacted with the radicals, which initiated the copolymerization of MMA monomer, on the PTFE surface was carried out by measuring the decrease of absorbance at 520 nm assigned to be DPPH. A calibration curve for the absorbance versus DPPH concentration was obtained by using a toluene solution containing DPPH of known concentration.[16]

The grafting ratio increases with an increase in the milling (mechanically fractured samples) or copolymerization time (γ-ray-irradiated samples) (Table 1).

The average degree of polymerization for the tethered PMMA chain, D_P, was calculated from the grafting ratio and the tethered point concentration.

We estimated a measure of the radius of gyration for the tethered polymer chain, assuming a Gaussian chain for the polymer chain and carbon−carbon bond length (b), 1.53 Å, as the effective bond length, for simplicity.

The mean square end-to-end distance for a Gaussian chain is given by

$$\langle R^2\rangle = Nb^2$$

where N is the number of bonds and b is the bond length. The mean square radius of gyration is given by

$$\langle S^2\rangle = \langle R^2\rangle/6 = Nb^2/6$$

In the case of the PMMA chain, as $N = 2D_P - 1$,

$$\langle S^2\rangle = (2D_P - 1)b^2/6$$

where D_P is an average degree of polymerization.

$2\langle S^2\rangle^{1/2}/A^{1/2}$ is used to estimate whether one tethered polymer chain can contact with neighbor chains or not, where $A^{1/2}$ is the distance from one tethered point to neighboring tethered points. If $2\langle S^2\rangle^{1/2}/A^{1/2}$ is smaller than 1.0, each of the tethered chains cannot contact. If $2\langle S^2\rangle^{1/2}/A^{1/2}$ is larger than 1.0, some tethered polymer chains can contact and entangle with neighbor chains.

(b) Dependence of Molecular Motion of Tethered PMMA Chains on Grafting Ratio. (1) Characteristics of ESR Spectra. Figure 3 shows an example of the ESR spectrum of spin-labeled PMMA tethered on the PTFE surface (PTFE/MMA(4h)) observed at 333 K (B) in comparison with the spectrum of the PMMA homopolymer (S-PMMA) (A). The fast component remarkably appears in the spectrum (B), whereas only one slow component is observed in the spectrum (A) and the extreme separation width for the slow component in (B) is smaller than that in (A). Figure 4 shows the temperature dependence of the extreme separation width for PTFE/MMA(4h) (open circles) in comparison with that for S-PMMA (solid circles). The characteristic differences between the results for both samples are found as follows:

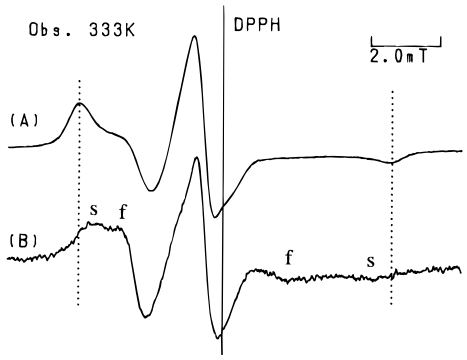

Figure 3. ESR spectra of S-PMMA (A) and PTFE/MMA(4h) (B) observed at 333 K. Fast and slow components are indicated by "f" and "s", respectively.

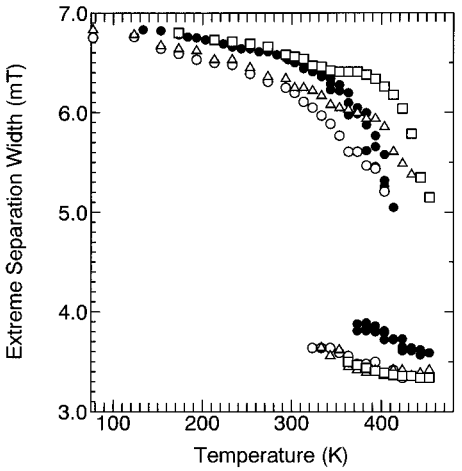

Figure 4. Temperature dependencies of the extreme separation width for PTFE/MMA(4h) (○), PTFE/MMA(8h) (△), PTFE/MMA(24h) (□), and S-PMMA (●).

(1) The fast component for PTFE/MMA(4h) appears at lower temperature than for S-PMMA.

(2) The extreme separation width of the slow component for PTFE/MMA(4h) is smaller than that for S-PMMA below $T_{5.0mT}$(410 K).

(3) The extreme separation width of the fast component for PTFE/MMA (4h) is smaller than that for S-PMMA.

These facts suggest that the PMMA chains tethered on the PTFE surface, with 0.1% grafting ratio, have higher mobility than the PMMA chains located on the

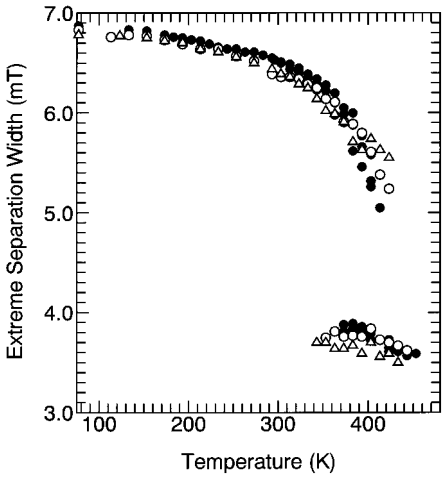

Figure 5. Temperature dependencies of the extreme separation width for γ-PTFE/MMA(2h) (△), γ-PTFE/MMA(6h) (○), and S-PMMA (●).

surface of PMMA homopolymer and have a large space around the tethered chains.

Two-component spectra are observed in a wide temperature range for PTFE/MMA(4h). This is a reflection of a broad distribution of correlation times arising from a heterogeneous structure of the tethered chains. For example, the distributions of molecular weight, segmental density, and PMMA−PTFE interaction of the tethered chains can be considered to be broad.

In Figure 4, variations of extreme separation with temperature for PTFE/MMA(8h) and PTFE/MMA(24h) are also shown. In the slow component for the PTFE/MMA samples, the transition temperature, $T_{5.0mT}$, shifts to the high-temperature side with an increase in grafting ratio, and the $T_{5.0mT}$s for PTFE/MMA(8h) and -(24h) are ca. 40 K higher than that for the PMMA homopolymer (S-PMMA). On the other hand, the temperature dependencies (Figure 5) for the γ-PTFE/MMA samples having a high grafting ratio are similar to those for S-PMMA, but the transition temperatures of the slow component are still ca. 10 K higher than that of S-PMMA. This fact suggests that the tethered polymer chains still have a small interaction with PTFE chains and the molecular mobility of the tethered polymer chains is a little bit higher than that of the PMMA molecules located on the PMMA surface.

(2) Transition Temperatures. In order to describe the dependence of the molecular motion of the tethered chains on grafting ratio (GR), two transition temperatures, T_L and T_H, were estimated. The lower T_L is where the sharp ^{14}N isotropic triplet spectrum first appears as the sample is warmed, while the upper T_H is where the broad spectrum identified with the anisotropic pattern finally disappears. The difference between T_L and T_H, ΔT, was also estimated as a measure of a distribution of molecular mobility. The characteristic temperatures, T_L and T_H, were defined as follows: Figure 6 shows the ESR spectrum of S-PMMA observed at 383 K. The amplitudes of I_f and I_s indicated in the figure are estimated as a measure of the intensities of the fast and slow components, respectively. The normalized intensities, I_f/S and I_s/S, are plotted against observation temperatures (Figure 7), where S means the total intensity of the spectrum estimated from the second moment of the derivative spectrum. I_f/S increases and I_s/S decreases with an increase in temperature. The temperatures extrapolated to zero of I_f/S and I_s/S by least-squares fitting can be regarded as T_L and

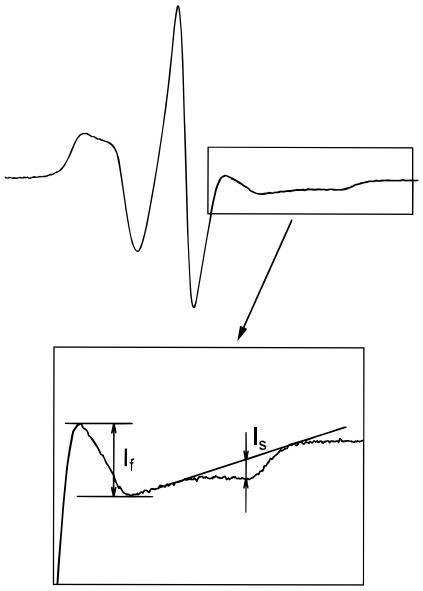

Figure 6. ESR spectrum of S-PMMA observed at 383 K. The spectrum in the bottom square shows the magnified spectrum of the upper square. I_f and I_s indicate the intensities of the fast and slow components, respectively.

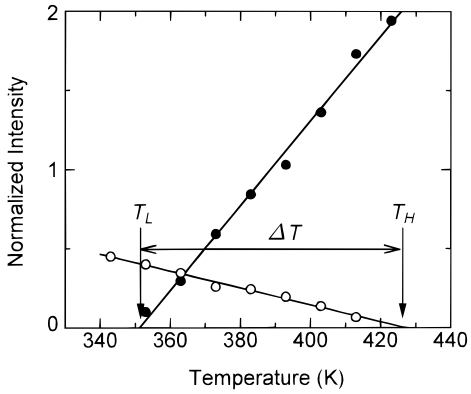

Figure 7. Example of two transition temperatures, T_L and T_H, and the difference ΔT. The normalized intensities, I_f/S and I_s/S, are shown with solid and open circles, respectively.

T_H as shown in Figure 7, respectively. The two transition temperatures for all grafted samples were estimated by the same method.

The obtained T_H and ΔT are plotted against weight fraction of PMMA (Figure 8). The T_H increases, has a maximum value around 3% grafting ratio, corresponding to 2.9% of the fractional amount of PMMA, and decreases toward the T_H of S-PMMA. The ΔT, which is a measure of distribution of molecular motion, also goes through a maximum around 3% grafting ratio and decreases with a decrease in grafting ratio toward the ΔT of S-PMMA.

Case 1, GR = 0.1%. In the case of 0.1% grafting ratio, T_H is very low as shown in Figure 8. Moreover, the extreme separation width in the fast component is more narrow than for S-PMMA as shown in Figure 4. When the grafting ratio is 0.1%, the tethered PMMA chain cannot contact with neighboring chains because the range of $2\langle S^2\rangle^{1/2}/A^{1/2}$ (Table 1) is smaller than 1.0. Therefore, the intermolecular interaction between the copolymer chains can be neglected and the PMMA copolymer chains have a very large space around themselves as shown in Figure 9. The interaction energy between tethered PMMA chains and PTFE chains is very low because of an immiscibility of both

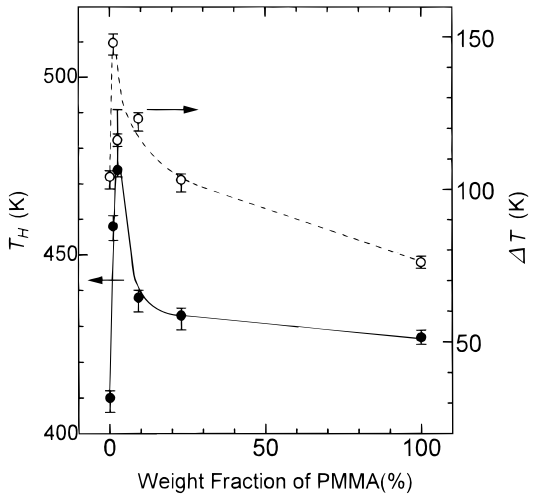

Figure 8. Dependencies of T_H and ΔT on weight fraction of PMMA.

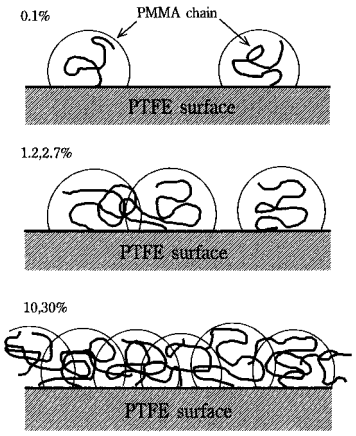

Figure 9. Schematic illustration of the PMMA chains tethered on the PTFE surface: (Top) At 0.1% grafting ratio, the tethered PMMA chains cannot touch and entangle with neighbor chains. The tethered chains have a very large space around themselves. (Middle) At 1.2 or 2.7% grafting ratio, the tethered chains still have a large space around themselves and some tethered chains entangle. (Bottom) At 10 or 30% grafting ratio, the tethered chains almost cover the PTFE surface.

chains. The tethered chain begins to protrude from the PTFE surface when the PMMA chain has a low thermal energy equal to the low interaction energy. Consequently, the molecular mobility of the tethered PMMA chain becomes very high. These facts reflect the extremely low segmental density of the PMMA chains.

Case 2, 0.1% ≤ GR ≤ 3%. In the range of grafting ratio lower than 3%, T_H drastically increases with an increase in grafting ratio (Figure 8). It can be considered that the segmental density of the tethered PMMA chains should increase drastically with an increase in grafting ratio and the molecular motion of these chains should become restricted. The T_H of the tethered PMMA chains is higher than that of S-PMMA. When the grafting ratio is ca. 1.2%, the tethered PMMA chain can begin to contact and entangle with neighboring chains because $2\langle S^2\rangle^{1/2}/A^{1/2}$ is nearly equal to 1.0 (Table 1). Some segments of the tethered PMMA chains adsorb on the PTFE surface like train segments adsorbed on a silica surface[17] because of the entanglements of the copolymer chain (Figure 9). The tethered PMMA chains strongly interacted with the PTFE chains should give rise to a higher transition temperature than that of S-PMMA as shown in Figures 4 and 8. However, some parts of low segmental density (nonentangled polymer chains) still exist in these systems (Figure 9). The nonentangled polymer chains still have a very high mobility reflected on a narrowing of the extreme separation width in the fast component as shown in Figure 4. The ΔT increases with an increase in grafting ratio. This reflects that the amount of the PMMA segments adsorbed on the PTFE surface increases and the PMMA chains have a wider distribution of molecular mobility.

Case 3, 3% ≤ GR. In the range of grafting ratio higher than 3%, the T_H of the tethered PMMA chains gradually decreases and approaches that of S-PMMA with an increase in grafting ratio. The T_L of the tethered PMMA chains is lower than that of S-PMMA, and the extreme separation width of the tethered chains is slightly more narrow than that of S-PMMA. These facts suggest that the distributions of molecular mobility are still wider than the distribution of S-PMMA. However, Figures 5 and 8 indicate that the molecular mobility of the tethered PMMA chains should approach that of S-PMMA with an increase in the grafting ratio. When the grafting ratio is 10 or 30%, the tethered PMMA chains almost cover the PTFE surface (see $2\langle S^2\rangle^{1/2}/A^{1/2}$ in Table 1) and the surface profile of the tethered PMMA chains should be close to that of PMMA homopolymer chains as illustrated in Figure 9. The spin-labeled sites are located near the surface of the tethered PMMA chains because the spin-labeling reaction was carried out in methanol. Therefore, the temperature dependencies as shown in Figure 5 reflect the surface molecular motion of the tethered PMMA chains and are similar to the result of S-PMMA, and these dependencies are still affected by the small amounts of nonentangled and adsorbed PMMA segments.

Conclusions

We could estimate the surface molecular motion of PMMA by spin-labeling (ESR). The molecular mobility of PMMA chains near a surface proved to be higher than that in the bulk of PMMA homopolymer.

The molecular motion of PMMA chains tethered on the PTFE surface strongly depended on the grafting ratio of the copolymer chains. The tethered PMMA chains without contact with neighboring chains had a very large space around themselves and had a very high mobility because of an extremely low segmental density when the grafting ratio was 0.1%. The tethered PMMA chains entangled with neighboring chains were adsorbed on the PTFE surface and strongly interacted with the PTFE chains when the grafting ratio was 2.7%. The transition temperature of the tethered PMMA chains was higher than that of S-PMMA. Both the transition temperature and distribution of the tethered PMMA chains approached those of S-PMMA with further increasing grafting ratio.

References and Notes

(1) Shiotani, M.; Sohma, J. *Polym. J.* **1977**, *9*, 283.
(2) Shiotani, M.; Sohma, J.; Freed, J. H. *Macromolecules* **1983**, *16*, 1495.
(3) Bullock, A. T.; Cameron, S. C.; Krajewski, V. *J. Phys. Chem.* **1976**, *80*, 1972.
(4) Tsay, F. D.; Gupta, A. *J. Polym. Sci., Part B: Polym. Phys.* **1970**, *25*, 589.
(5) Shimada, S.; Hori, Y.; Kashiwabara, H. *Macromolecules* **1988**, *21*, 2107.
(6) Sakaguchi, M.; Yamaguchi, T.; Shimada, S.; Hori, Y. *Macromolecules* **1993**, *26*, 2612.
(7) Sakaguchi, M.; Shimada, S.; Hori, Y.; Suzuki, A.; Kawaizumi, F.; Sakai, M.; Bandow, S. *Macromolecules* **1995**, *28*, 8450.

(8) Shimada, S.; Suzuki, A.; Sakaguchi, M.; Hori, Y. *Macromolecules* **1996**, *29*, 973.
(9) Sakaguchi, M.; Sohma, J. *J. Polym. Sci., Polym. Phys. Ed.* **1975**, *13*, 1233.
(10) Sakaguchi, M.; Sohma, J. *J. Appl. Polym. Sci.* **1978**, *22*, 2915.
(11) Mukherjee, A. K.; Gupta, B. D. *J. Macromol. Sci., Chem.* **1983**, *A19* (7), 1069.
(12) Baltzly, R.; Berger, I. M.; Rothstein, A. A. *J. Am. Chem. Soc.* **1950**, *72*, 4149.
(13) Veksli, Z.; Moller, W. G.; Thomas, E. L. *J. Polym. Sci., Polym. Symp.* **1976**, *No. 54*, 299.
(14) Mayes, A. M. *Macromolecules* **1994**, *27*, 3114.
(15) Kajiyama, T.; Tanaka, K.; Takahara, A. *Macromolecules* **1995**, *28*, 3482.
(16) Ito, Y.; Inaba, M.; Chung, D. J.; Imanishi, Y. *Macromolecules* **1992**, *25*, 7313.
(17) For example: (a) Hommel, H.; Legrand, A. P.; Tougne, P.; Balard, H.; Papirer, E. *Macromolecules* **1984**, *17*, 1578. (b) Sakai, H.; Imamura, Y. *Bull. Chem. Soc. Jpn.* **1987**, *60*, 1261.

MA960718S